JOURNAL OF Applied Polymer SCIENCE

Evaluation of the Fracture Behaviors of Multilayered Propylene–Ethylene Copolymer/Polypropylene Homopolymer Composites with the Essential Work of Fracture

Guansong He, Fengshun Zhang, Liang Huang, Jiang Li, Shaoyun Guo

State Key Laboratory of Polymer Materials Engineering, Polymer Research Institute of Sichuan University, Chengdu 610065, China

Correspondence to: J. Li (E-mail: li_jiang@scu.edu.cn) or S. Guo (E-mail: nic7702@scu.edu.cn)

ABSTRACT: As one of the most appropriate techniques for evaluating the fracture behavior, the essential work of fracture (EWF) was introduced to investigate the fracture toughness of multilayered composites. Propylene–ethylene copolymer (CPP)/polypropylene homopolymer (HPP) alternating multilayered composites with 2–128 layers were prepared though multilayered coextrusion. Polarized optical microscopy photographs revealed that the CPP and HPP layers aligned alternately vertical to the interfaces and continuously parallel to the extrusion direction. The dichroic Fourier transform infrared spectroscopy results showed that the coextrusion sheet had a preferential orientation parallel to the melt flow direction (MD); this caused crack propagation along the blunted MD and the necking ligament section. After heat treatment, the orientation parallel to the MD could been largely eliminated, and the crack propagated in a stable manner. The specific essential work of fracture (w_e) of the multilayered composite was higher than that of the blend; this indicated a higher resistance of crack propagation. The number of layers had little effect on the toughness of the multilayered composites. © 2014 Wiley Periodicals, Inc. J. Appl. Polym. Sci. **2014**, *131*, 40574.

KEYWORDS: extrusion; mechanical properties; morphology; polyolefins

Received 29 December 2013; accepted 7 February 2014
DOI: 10.1002/app.40574

INTRODUCTION

The synergistic combination of two or more materials in a layered structure can enhance the overall properties of a material.[1] These layered composites are structured to obtain or enhance the desirable physical properties of each component without the sacrifice of other important properties. To obtain layered-structure polymer composites, microlayer coextrusion has been introduced to manufacture more and more layered polymer films and sheets in recent years.[2–5] Layered products have had an increasing presence in the plastic business.[6,7]

The mechanical properties of polymer composites are strongly dependent on their composition and morphology. Compared with common structure, the layered structure has better mechanical properties. Simulation results obtained by some theoretical models, such as the equivalent box, have indicated that the mechanical properties, including the modulus, yield strength, and tensile strength, of layered structure are higher than those of a dispersed, cocontinuous structure.[8–11] Kolarik[10,11] ascribed this enhancement in the mechanical properties of a layered morphology to its best phase continuity in the direction of the acting force. Hiltner and coworkers[12–14] found that microlayered polycarbonate and styrene–acrylonitrile copolymer materials could present ductile fracture behavior because of the interaction between the crazing and shear-banding that were formed at the interface. However, very few studies have covered the fracture toughness of layered-structure materials.

For the fracture and toughening characterization of polymer composites, empirical tests, such as impact tests or tensile tests, are commonly used. However, these empirical methods give test results that are dependent on the specimen geometry and test configuration and, therefore, are not representative of the true material behavior.[15] Fracture mechanics analysis, on the other hand, can give a true measure of the toughness and crack-resistance behavior. Within the frame work of fracture mechanics theories, the essential work of fracture (EWF) method, first proposed by Broberg[16] and then developed by Cotterell and

Additional Supporting Information may be found in the online version of this article.

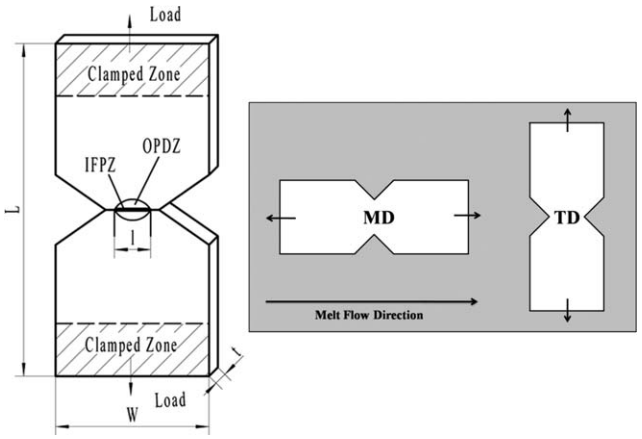

Figure 1. DDENT used in the EWF test and schematic of the testing directions. The W and L indicate the width and length of DDENT specimen, respectively.

coworkers,[17,18] Karger–Kocsis and coworkers,[19–22] and Mai and coworkers,[23–25] has been used extensively as the most appropriate technique for studying the fracture behavior of a wide range of polymeric materials.

The fundamental concept of the EWF method is based on the energy partition, which partitions the total fracture energy (W_f) into two components: the essential work of fracture (W_e) and the nonessential, or plastic, work of fracture (W_p). W_e is the energy involved in the creation of new surfaces during crack propagation (the inner fracture process zone), and W_p collects the volume energy dissipated during the plastic deformation process (the outer plastic deformation zone).[26] These zones are schematized in Figure 1 for a deeply double-edge notched tension specimen (DDENT) specimen. W_f can be expressed as follows:

$$W_f = W_e + W_p = w_e lt + w_p \beta l^2 t \quad (1)$$

$$w_f = W_f / lt = w_e + \beta w_p l \quad (2)$$

where l is the ligament length, t is the specimen thickness, β is the shape factor that is associated with the dimension of the plastic zone, and w_e and w_p are the specific essential work of fracture and specific nonessential work of fracture or specific plastic work, respectively. w_e has been shown to be a material property and is independent of the specimen geometry.[27] It can be used to characterize the fracture toughness. βw_p is the specific nonessential work of fracture;[28] however, it is not considered a material constant, and it depends on the shape of the plastic zone surrounding the crack, the specimen geometry, testing speed, and so on. A linear relationship is expected between the specific work of fracture (w_f) and l according to eq. (2). The positive intercept of this line with the w_f axis gives w_e, and its slope gives βw_p.[29,30]

Gámez-Pérez et al.[8] investigated the fracture behavior of coextruded polypropylene sheets using the EWF method. The results show that coextrusion with an ethylene–propylene copolymer could improve the fracture behavior of the polypropylene extruded sheets. However, further detailed work has not been continued, such as work on the fracture toughness differences of layered structures and conventional blended structures, and the effects of the layer number on the fracture behavior of a multilayered structure for conventional coextrusion is an invalid method for constructing laminar polymeric materials with high layer numbers.

In this study, we studied in detail the differences in the fracture toughness between conventional and layered structures by means of the EWF method. Multilayered propylene–ethylene copolymer (CPP)/polypropylene homopolymer (HPP) composites were prepared by a multilayered coextrusion technology developed in our laboratory, and the number of layers could amount to thousands when the number of layer multiplying elements (LMEs) was increased. Thus, the effect of the number of layers on the fracture toughness of multilayered-structure materials was investigated in this study.

EXPERIMENTAL

Materials

The materials used in this study were a CPP and one HPP. The CPP was EPS30R from Du Shan Zi Petroleum Chemical Co., Ltd. (China), which consisted of 6.5 wt % ethylene and had a melt flow rate (measured at 230°C and 2.16 kg) of 1.5 g/10 min. The HPP was T38F from Lanzhou Petrochemical Co. (China); it had a melt flow rate (measured at 230°C and 2.16 kg) of 3.0 g/10 min.

Specimen Preparation

Multilayered sheets consisting of alternating CPP and HPP layers were extruded with a multilayered coextrusion system developed in our laboratory, as described previously.[4] The 2-, 8-, 16-, 32-, 64-, and 128-layer specimens were extruded by the variation of the number of LMEs. All of the multilayered sheets were about 0.5 mm thick and 50 mm wide after cooling. Without LMEs, neat CPP and LDPE sheets were also prepared respectively by one single-screw extruder (SJ-30) and had the same dimensions as the multilayered specimens. The temperature profile was in the range of 150–200°C for CPP and HPP. The temperatures of the LMEs and coextrusion block were both 200°C. For comparison, conventional blended CPP/HPP specimens were also prepared as sheets with the same dimensions. HPP and CPP with the same proportions as those in the multilayered structure were first mixed in a high-speed mixer and then extruded with an extruder of multilayered coextrusion system to retain the same history as corresponding multilayered composites.

To study the effect of orientation on the testing, the DDENT specimens were obtained in the melt flow direction (MD) and transverse direction (TD), respectively, as depicted in Figure 1. Next, to investigate the effect of layered structure on the fracture toughness, the orientation structure caused by processing would be eliminated by heat treatment. Prior preparation of DDENT sample, the sheet had been maintained at 175°C for 10 min, and then cooled to room temperature. At the temperature of 175°C, the orientation structures of CPP and HPP which included the crystalline phase and amorphous phase could melt.

The DDENT specimens (length × width × thickness = 100 × 35 × 0.5 mm) shown in Figure 1 were cut from the sheets. Sharp precracks on both sides of the specimens were made with a fresh razor blade. To meet the plane stress conditions, their

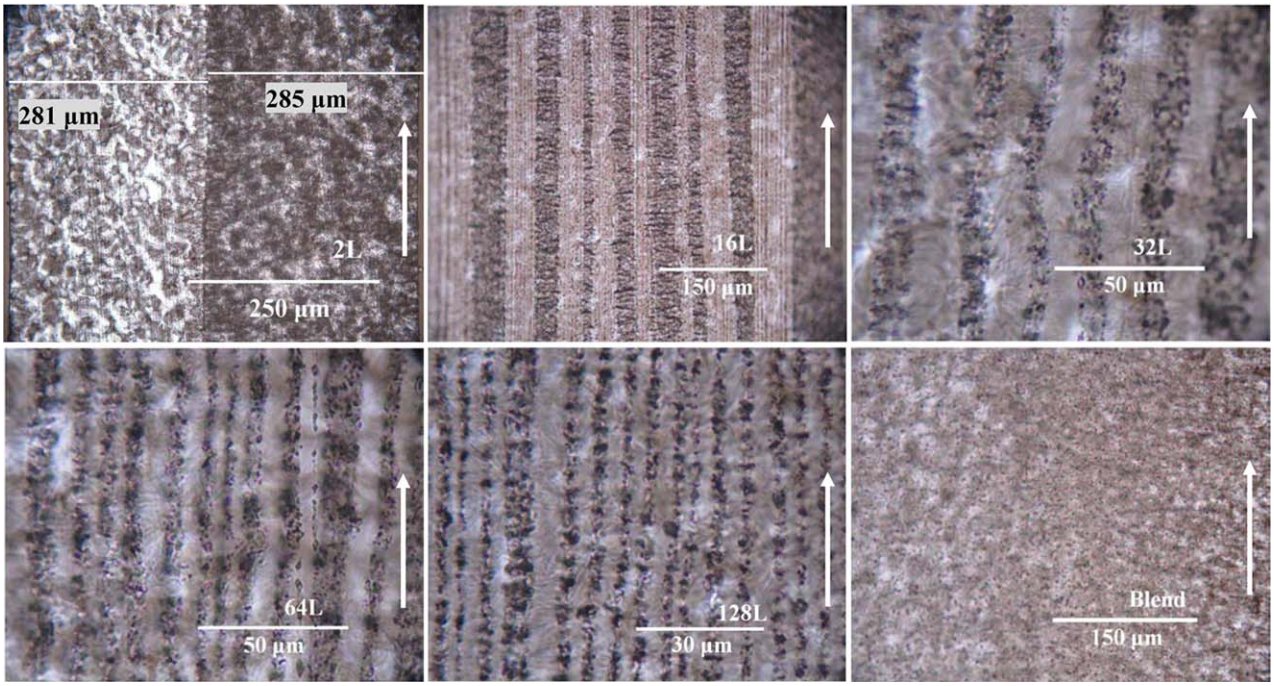

Figure 2. POM micrographs of the multilayered and conventional CPP/HPP composites. The arrow indicates the extrusion direction. [Color figure can be viewed in the online issue, which is available at wileyonlinelibrary.com.]

ligament range was limited ($3t < l < w/3$).[31] The w indicates the width of DDENT specimen. The l and thickness values of all of the specimens were measured with a microscope and a vernier caliper, respectively.

Polarized Optical Microscopy (POM)

A POM instrument (BX51, Olympus, Japan) equipped with a video camera was used to observe the multilayered morphologies of the composites. The thin slice for testing, which was about 10 μm thick, from the specimen along the extrusion direction was obtained by a microtome. We obtained the volume fractions of the CPP and HPP by measuring the thicknesses of the CPP and HPP layers. As all of the multilayered sheets were prepared with the same processing conditions, including the same temperature and extruder speed, the proportions of two components did not change much with the number of layers. The two-layer specimen was selected as an example for the estimation of the layer thickness because of it was simple and easy to observe and measure. The thicknesses of the CPP and HPP layers measured by the pixel measurements of the POM image for the two-layer specimen are shown in Figure 2, and the calculated volume fractions of CPP and HPP were 50.3 and 49.7%, respectively. The volume fractions of the CPP and LDPE obtained by the measurement of the thicknesses for the other samples are listed in Table I.

Fourier Transform Infrared (FTIR) Spectroscopy

For FTIR measurements, a Nicolet iS10 FTIR instrument from Thermo Fisher Scientific at a resolution of 2 cm^{-1} with an accumulation of 128 scans was used. Polarization of the beam was done with a zinc selenide wire grid polarizer. This measurement is based on the absorption of IR light at certain frequencies corresponding to the vibration modes of atomic groups present within the molecule. In addition, if a specific vibration is attributed to a specific phase, the orientation within that phase can be determined.[32] If the films are oriented, the absorptions of plane-polarized radiation by a vibration in two orthogonal directions, specifically, the directions parallel and perpendicular to a reference axis (MD), should be different. The ratio of these two absorption values is defined as the dichroic ratio (D):

$$D = \frac{A_{\parallel}}{A_{\perp}} \tag{3}$$

where $A_{\parallel}$ is the absorption parallel to a specific reference axis and $A_{\perp}$ is the absorption perpendicular to a specific reference axis. The Herman orientation function (F) of this vibration is obtained according to the following equation:

$$F = \frac{2}{3\cos^2(\alpha - 1)} \times \frac{D-1}{D+2} \tag{4}$$

where α is the angle that the transition moment makes with the polymer chain axis, which was taken to be equal to 18°, as mentioned in ref. 33.

Table I. Contents of CPP and HPP in the Multilayered Composites

Specimen	Volume fraction of CPP (%)	Volume fraction of HPP (%)
2L	50.3	49.7
8L	50.4	49.6
16L	50.2	49.8
32L	50.1	49.9
64L	49.9	50.1
128L	49.4	50.6

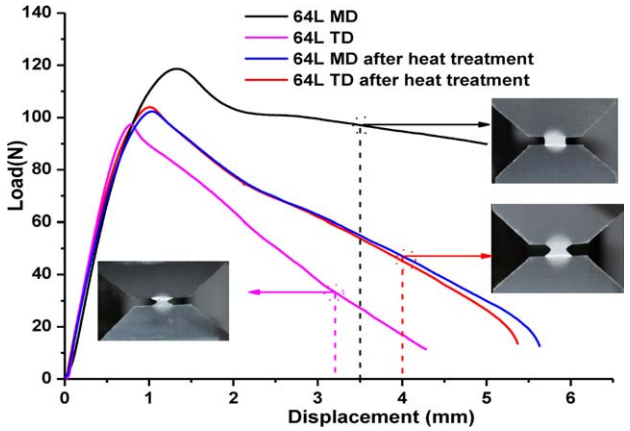

Figure 3. Load–displacement curves of the 64L DDENT specimens with and without heat treatment in different testing directions and photographs taken during EWF testing. [Color figure can be viewed in the online issue, which is available at wileyonlinelibrary.com.]

For polypropylene, the absorption at a wave number of 998 cm^{-1} was attributed to the crystalline phase (*c* axis), whereas the absorption at a wave number of 972 cm^{-1} was due to the contributions of both the crystalline and amorphous phases. From the former absorption, the orientation of the crystalline phase (F_c) was determined, whereas from the latter, the average orientation function (F_{avg}) was obtained.[34]

EWF Fracture Test

The EWF tests of the DDENT specimens were performed on an Instron 5567 tension machine (Canton, MA) with a 1-kN load cell at room temperature (23°C). The crosshead speed was set at 3 mm/min. The load–displacement curves were recorded, and the energy absorbed until failure was calculated by computer integration of the load–displacement curves.

Scanning Electron Microscopy (SEM)

To observe the interfacial interaction between the CPP and HPP layers during the EWF test, the fractured specimens were cryofractured in liquid nitrogen first, and then, the fracture surfaces were coated with a layer of gold in a vacuum chamber for conductivity. Finally, they were examined by SEM (JSM-5900LV, Japan) at an accelerating voltage of 20 kV.

RESULTS AND DISCUSSION

Phase Morphology

Figure 2 shows the POM micrographs of the CPP/HPP multilayered (2L, 16L, 32L, 64L, and 128L) and conventional composites. The sample code "NL" indicates the multilayered sample with the layer number of N. The darker layers in the images belonged to CPP, which had a lower crystallinity compared to HPP, whereas the whiter layers belonged to HPP. We found that the all of the multilayered specimens had a layered morphology, where the CPP and HPP layers aligned alternately vertical to the interfaces and continuously parallel to the extrusion direction. Although the thicknesses of different CPP or HPP layers that existed in the same specimen were not always symmetrical in thickness, the layer continuity was relatively constant. On the other hand, the conventional blend had a morphology similar to the cocontinuous structure, and obviously, the individual phase continuity in the extrusion direction became lower.

Effect of the Orientation on the Fracture Behavior

The load–displacement curves of the 64L DDENT specimens in different directions during the EWF tests are shown in Figure 3. We noticed that the fracture behaviors of the 64L specimens without heat treatment presented huge differences in the MD and TD. For testing in the MD, instead of steady crack propagation after the maximum load, the ligament section yielded, and the specimen started to become blunt at the notches. This blunting phenomenon prevented crack propagation, and the ligament section continued with the necking. The blunting and necking prevented the applicability of the EWF method.[31,35] In the contrary, for the TD, the crack propagated very quickly after the yielding of the ligament and showed a relatively low resistance of crack propagation. Similar fracture behaviors were observed for all of the extrusion sheets. The fracture behaviors were strongly dependent on the testing direction.[8]

In our previous studies, the polymer could orientate along the MD because of the action of strong shear forces when it experienced multilayered coextrusion. Therefore, the previous phenomenon could possibly be interpreted in terms of a

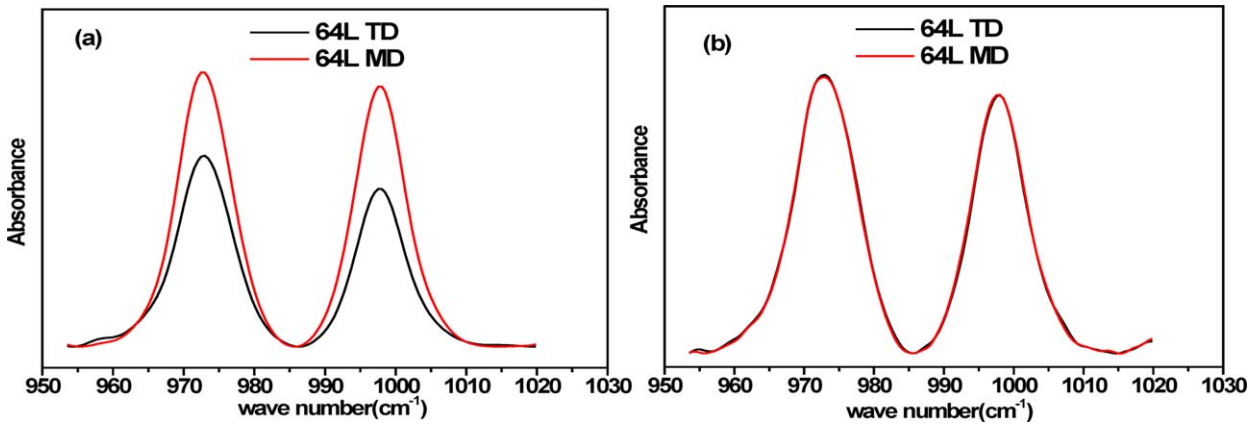

Figure 4. Polarizing IR ray spectra of the 64-layer CPP/HPP specimens for (a) extrusion sheets without heat treatment and (b) extrusion sheets with heat treatment. [Color figure can be viewed in the online issue, which is available at wileyonlinelibrary.com.]

Table II. Degree of Orientation for the 64-Layer Specimens with and Without Heat Treatment Along the MD

Specimen	D_c	F_c	D_{avg}	F_{avg}
64L without heat treatment	1.663	1.175	1.369	0.711
64L with heat treatment	1.011	0.024	1.000	0

preferential orientation parallel to the MD. The dichroic FTIR technique was used to measure the orientation of the extrusion sheet along the MD. The absorption anisotropy of the 64-layer CPP/HPP specimen without heat treatment is shown in Figure 4(a). The strength of the peaks at 998 and 972 cm^{-1} in the MD was higher than that in TD. The calculated values of the orientation functions for the 64-layer sheets are listed in Table II. D_c represents the dichroic ratio of the crystalline phase, whereas D_{avg} represents the dichroic ratio of both the crystalline and amorphous phases. F_c represented the Herman orientation function of the crystalline phase, whereas F_{avg} represents the Herman orientation function of both the crystalline and amorphous phases. We found that the D_c and D_{avg} values were larger than 1, whereas the F_c and F_{avg} values were larger than 0. This revealed a high degree of orientation along the MD. Moreover, the orientation structure was responsible for the strong fracture anisotropy during EWF testing. This was because the preferential orientation along the MD could hold up the crack propagation and result in a great amount of energy absorption, and the ligament section continued with the necking. However, in the tests performed in the TD, as the crack propagated along the oriented structures, the energy involved in the fracture process was much lower.

As the necking caused by orientation could prevent the applicability of the EWF method, it was necessary to eliminate orientation through heat treatment. Figure 4(b) shows the absorption anisotropy of the 64-layer CPP/HPP specimen after heat treatment. The absorption peaks parallel to the MD became close to those in the TD. The calculated values listed in Table II showed that the orientation parallel to the MD for the 64-layer sheet was largely eliminated after heat treatment. As a result, the fracture behaviors of the 64-layer composites with heat treatment presented little difference in the MD and TD during EWF testing, as shown in Figure 3. The curves revealed that the crack propagated in a stable manner, one of the necessary conditions that guarantee the validity of EWF testing.

Load–Displacement Curves

The load–displacement curves of the DDENT specimens of the CPP, HPP, multilayered, and conventional composites with heat treatment during EWF testing as a function of l are shown in Figure 5. For all of the materials, similar trends were observed. First, the load increased quickly with increasing displacement before the maximum load point. Then, a smooth and slow drop in the load

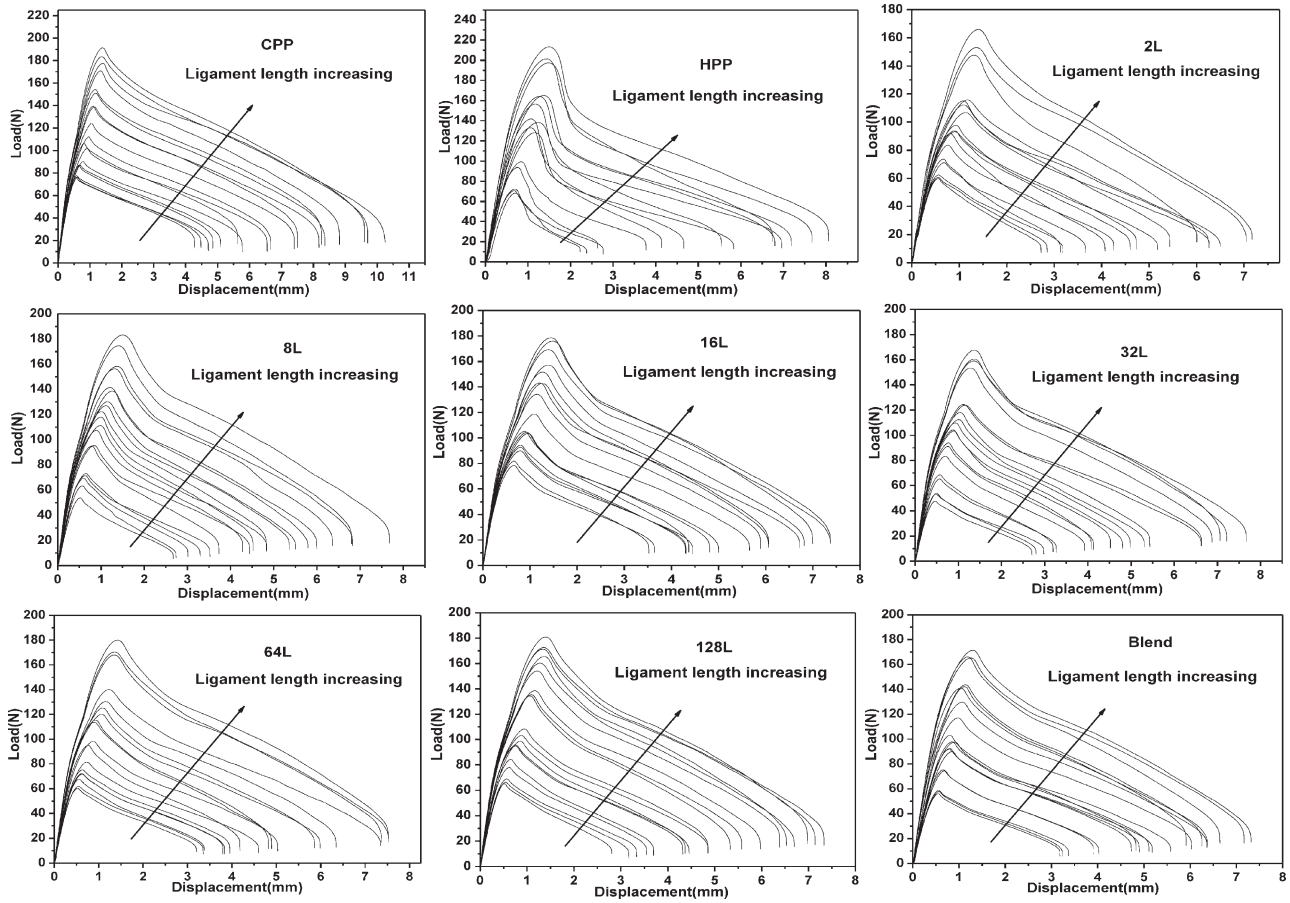

Figure 5. Load–displacement curves for CPP, HPP, and multilayered and conventional composites with heat treatment.

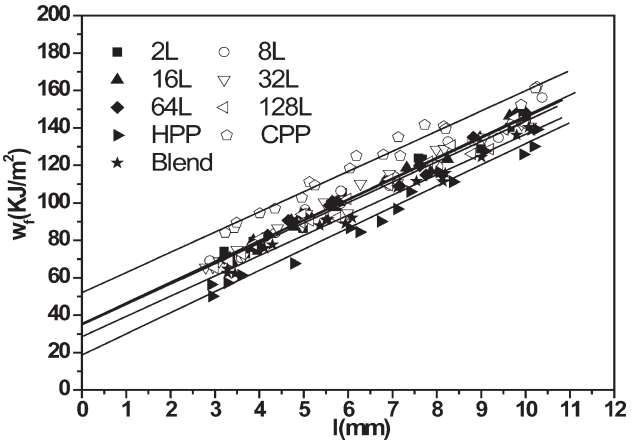

Figure 6. w_f versus l for the CPP, HPP, and multilayered and conventional CPP/HPP composites.

occurred, and the ligament began to yield. After the complete yielding of the ligament, the cracks began to propagate in a stable manner until the final fracture of the specimen. The curves for each group of specimens with the same composition showed excellent reproducibility. The maximum load and the displacement to failure increased regularly with increasing l, and each group of curves had a good self-similarity. This behavior ensured that the cracks propagated under similar stress, which was unchanged with l.[36] Therefore, the fracture behaviors of all of the DDENT specimens after the heat treatment described previously could absolutely satisfy the prerequisite for EWF analysis.[27]

Fracture Parameters of the EWF Testing

W_f was obtained by the integration of the load–displacement curves shown in Figure 5. The plots of w_f versus l of all of the DDENT specimens with heat treatment are shown in Figure 6. It was clear that all of the w_f–l diagrams gave very good linear relationships. The values of w_e and βw_p that were obtained from the interception and slope of the straight lines extrapolated to zero l, together with the regression coefficient, are listed in Table III. From the values listed in Table III, it was clear that the specific essential work of fracture (w_e) of CPP was obviously higher than that of HPP; this indicated that the crack propagation resistance of the former was higher than that of the latter. This was caused by the better toughness of CPP when the propylene copolymerized with ethylene. However, βw_p of CPP was a little lower than that of HPP; this indicated that less energy for plastic deformation was absorbed during the fracture process for CPP.

The w_e values of the conventional and multilayered composites were intervenient between the values of CPP and HPP. However, the w_e values of the multilayered blends were obviously higher than those of the conventional blends, although the proportions of the two components were the same in these composites. With increasing number of layers, the w_e values did not show significant differences for any of the multilayered specimens; this indicated that the effect of the number of layers on the fracture toughness of the multilayered specimens was very small.

For a binary composite, the upper band of the mechanical properties (Y; parallel model) is given by the rule of binary mixtures:[37]

$$Y = Y_1\phi_1 + Y_2\phi_2 \quad (5)$$

where Y_1 and Y_2 are the mechanical properties of components 1 and 2, respectively, and &phis;$_1$ and &phis;$_2$ are the volume fractions of components 1 and 2, respectively. This equation is applicable for models, such as alternating layered structure, in which the components are arranged parallel to the applied stress. In many previous articles,[11–14] it was found that the mechanical properties, including the modulus, yield strength, and tensile strength, of a layered structure were higher than those of a dispersed and cocontinuous structure because of its best phase continuity in the direction of the acting force. However, the evaluation of the fracture toughness parameters of multilayered materials with the parallel model has rarely been reported in the literature. According to eq. (5), the theoretical w_e values of the multilayered specimen are listed in Table III; these were very close to the experimental w_e values of the multilayered blends and indicated that the fracture toughness of the multilayered blends could meet the upper-band rule of binary mixtures. The phase continuity of the conventional blends in the direction of the acting force was much lower than that of multilayered blends; this caused a relatively lower w_e value. With increasing number of layers, the layered structure was not destroyed, and the phase continuity, along the acting force direction, did not change. Therefore, the w_e values actually did not show significant differences.

Table III. Fracture Parameters for the DDENT Specimens

Specimen	w_e (kJ/m^2)	βw_p (MJ/m^3)	R^2	Theoretical value of w_e
HPP	18.70	11.29	0.98	—
CPP	52.04	10.79	0.98	—
Blend	28.50	10.82	0.99	—
2L	35.17	11.07	0.98	35.49
8L	35.44	11.10	0.98	35.51
16L	35.39	11.04	0.99	35.45
32L	35.29	11.03	0.98	35.40
64L	35.37	11.09	0.99	35.35
128L	34.77	10.89	0.98	35.16

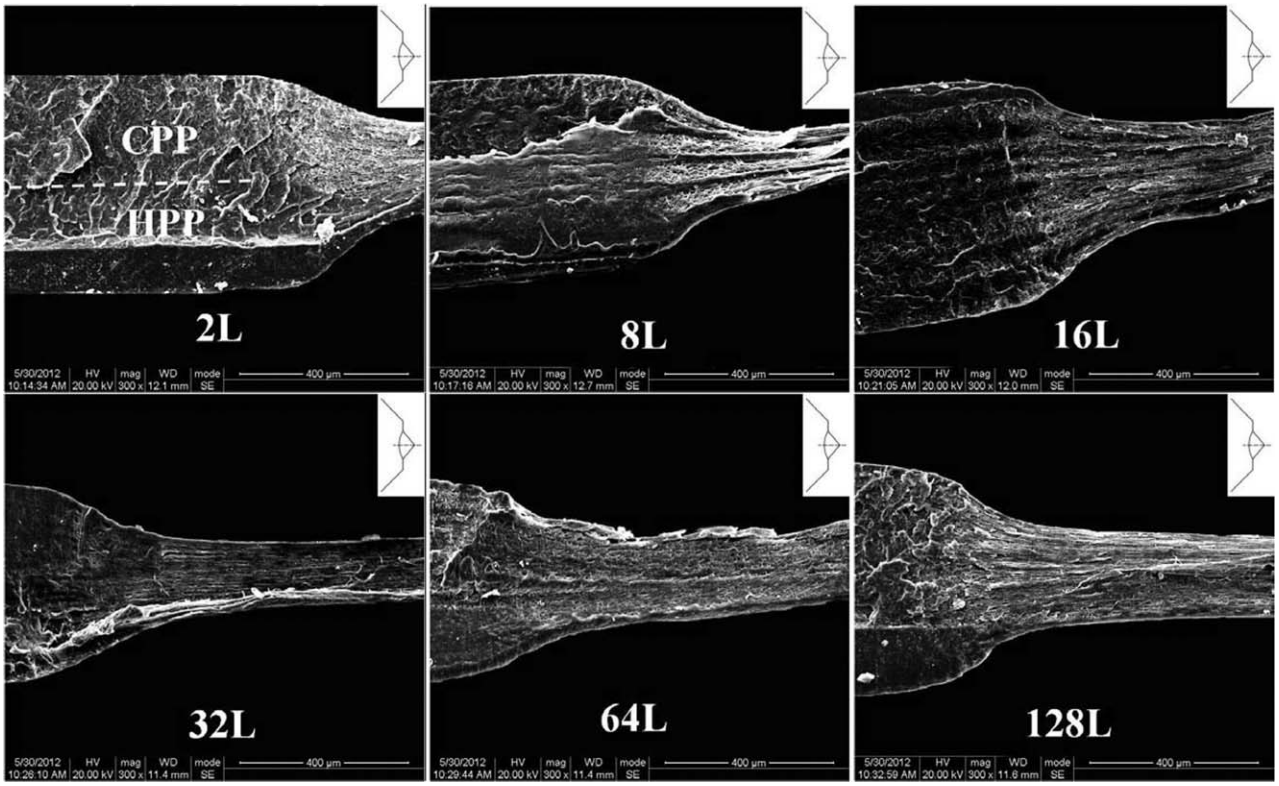

Figure 7. SEM micrographs of the multilayered specimens after fracture. The sketch in the upper right corner of each image indicates the area where the picture was taken.

The surface aspect of the tested specimens was observed with SEM. Figure 7 shows SEM micrographs of the multilayered CPP/HPP specimens, where the deformed CPP and HPP layers could be easily distinguished by the different plastic deformation surfaces. The CPP layer was a little whitish and rough, whereas the HPP layer surface was rather smooth. The layer interface could maintain integrity. In addition, there was no layer delamination phenomenon during the crack propagation for all of the multilayered specimens. This observation indicated that the crack propagated only through the ligament section and not at the layer interfaces. Therefore, the energy involved in the creation of new surfaces during the crack propagation was more or less for the specimens with different numbers of layers. The phase continuity became an essential factor affecting the fracture toughness.

Our other work[38] revealed that during the crack propagation of multilayered CPP/LDPE composites, interfacial delamination behavior could occur because of the weaker interface strength; this caused the absorbed surface energy to increase with the number of layers. Hence, w_e increased with the increasing number of layers.

Fracture Energy Partitioning

To determine the energy distribution during the fracture process and in which fracture stage the w_e value of the multilayered specimen was higher than that of conventional blend, a method of yielding work well accepted in the EWF literature,[27,28,39] was used in this study. With the peak of the load–displacement curves made as the cutoff point (see Figure 8), w_f can be partitioned into the specific work of fracture for yielding (w_y) and specific work of fracture for necking and subsequent fracture (w_n). Equation (1) can be rewritten as

$$w_f = w_y + w_n \tag{6}$$

$$w_y = w_{e,y} + \beta w_{p,y} l \tag{7}$$

$$w_n = w_{e,n} + \beta w_{p,n} l \tag{8}$$

where $w_{e,y}$ and $w_{e,n}$ are the parts of the specific essential work of fracture related to yielding and necking, respectively, and

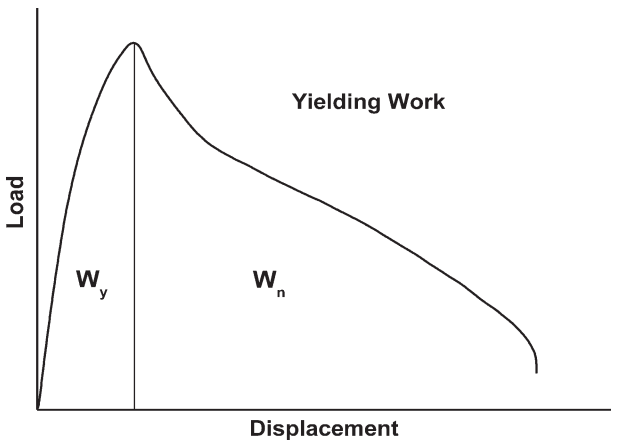

Figure 8. Load–displacement curve and energy partition method by yielding work.

Table IV. Constituting Terms for the EWF for the Multilayered and Conventional CPP/HPP Composites

Specimen	$w_{e,y}$ (kJ/m^2)	$\beta w_{p,y}$ (MJ/m^3)	R^2_y	$w_{e,n}$ (kJ/m^2)	$\beta w_{p,n}$ (MJ/m^3)	R^2_n
Blend	2.02	2.58	0.97	26.48	8.23	0.98
2L	5.03	3.03	0.78	30.14	8.04	0.93
8L	7.22	2.78	0.95	28.22	8.32	0.97
16L	5.01	2.90	0.98	30.38	8.13	0.98
32L	5.10	2.69	0.95	30.19	8.34	0.98
64L	3.69	2.77	0.96	31.68	8.32	0.96
128L	4.03	2.83	0.97	30.74	8.06	0.98

$\beta w_{p,y}$ and $\beta w_{p,n}$ are the yielding and necking and subsequent fracture components of the nonspecific essential work of fracture, respectively.

The results for splitting the essential and nonessential works of fracture as yielding and necking and subsequent fracture terms are given in Table IV; these values were obtained by the plotting of w_y and w_n versus l, as shown in Figure 9(a,b). The regression coefficient for necking and subsequent fracture (R^2_n) remained above 0.92, and the regression coefficient for yielding (R^2_y) remained mostly above 0.94. This indicated that the partition method was relatively applicable for the CPP/HPP composites.

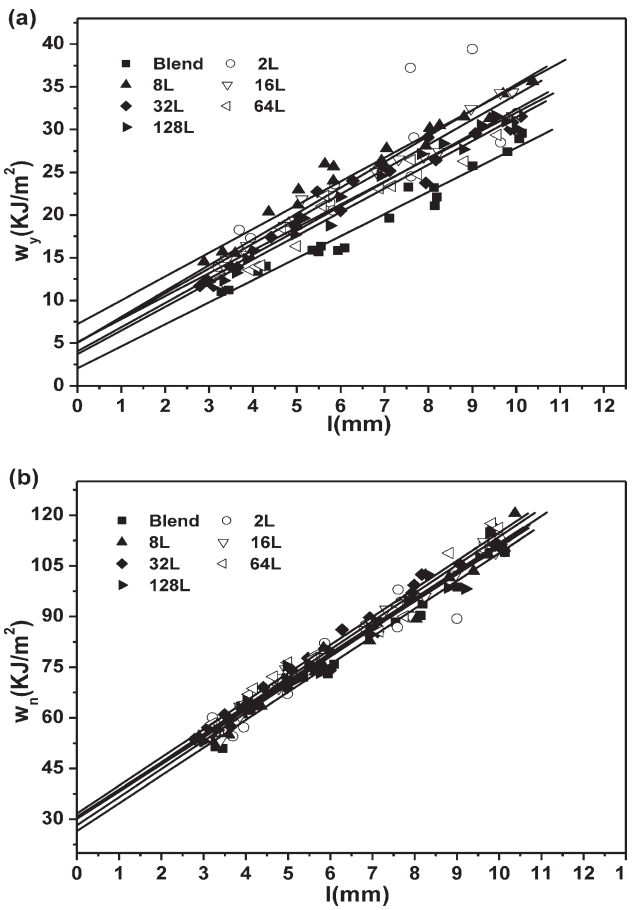

Figure 9. (a) Yielding and (b) necking w_f versus l for the multilayered and conventional CPP/HPP composites. The spots with different shapes represent the experimental data, whereas the straight lines are the fitting results.

From the results listed in Table IV, we found that for all of the specimens, $w_{e,y}$ was much lower than the corresponding $w_{e,n}$. A similar phenomenon was found for the plastic w_y and the corresponding term for necking and subsequent fracture. These results indicated that both w_e and βw_p in the whole fracture process for the multilayered and conventional composites were mostly determined by w_n. In addition, remarkable decreases in $w_{e,y}$ and $w_{e,n}$ were found for the conventional composites compared with the multilayered composites. This indicated that the effect of the morphological structure on the crack resistance in the yielding stage could not be neglected. Additionally, $w_{e,y}$ and $w_{e,n}$ did not change evidently with the number of layers. Therefore, for the multilayered specimens with a higher fracture toughness, sufficient attention should be paid to the values of both $w_{e,y}$ and $w_{e,n}$.

CONCLUSIONS

During crack propagation, the blunting and necking behaviors caused by the preferential orientation parallel to the MD prevented the applicability of the EWF method. After heat treatment at the temperature above the melting point, the orientation along the MD was eliminated, and the fracture behavior and toughness of the CPP, HPP, and multilayered and conventional CPP/HPP composites was successfully evaluated with the EWF method. The w_e value of the blend was lower than that of the multilayered specimen; this indicated that the multilayered specimen had a higher resistance of crack propagation. Moreover, in the whole fracture process, no delamination at the interfaces of the layers occurred. The crack propagated only through the ligament section. Therefore, the higher phase continuity became an essential factor causing the higher fracture toughness of the multilayered specimens. In addition, the number of layers had little effect on the toughness of the multilayered specimens. For the term of plastic deformation work, the βw_p values of the blend and all of the multilayered specimens did not show significant differences.

By partitioning the work of fracture for the blend and multilayered specimens studied, we found that the specific essential and plastic deformation work of fracture for necking and subsequent fracture ($w_{e,n}$ and $\beta w_{p,n}$) were much higher than the corresponding terms for yielding ($w_{e,y}$ and $\beta w_{p,y}$). A higher w_e value for the multilayered specimen compared with the conventional

blend was mainly achieved through the combination of both the $w_{e,y}$ value and $w_{e,n}$ value.

ACKNOWLEDGMENTS

The authors are grateful to the National Natural Science Foundation of China (contract grant numbers 50933004, 51073099, and 51121001), the Ministry of Education Priority Funding Areas (contract grant number 20110181130004), and the Program for New Century Excellent Talents in University (contract grant number NCET-10–0593) for their financial support of this work.

REFERENCES

1. Baer, E.; Hiltner, A.; Keith, H. *Science* **1987**, *235*, 1015.
2. Kerns, J.; Hsieh, A.; Hiltner, A.; Baer, E. *J. Appl. Polym. Sci.* **2000**, *77*, 1545.
3. Ania, F.; Baltá-Calleja, F. J.; Flores, A.; Michler, G. H.; Scholtyssek, S.; Khariwala, D.; Hiltner, A.; Baer, E.; Rong, L.; Hsiao, B. S. *Eur. Polym. J.* **2012**, *48*, 86.
4. Langhe, D. S.; Murphy, T. M.; Shaver, A.; LaPorte, C.; Freeman, B. D.; Paul, D. R.; Baer, E. *Polymer* **2012**, *53*, 1925.
5. Shen, J.; Wang, M.; Li, J.; Guo, S.; Xu, S.; Zhang, Y. *Eur. Polym. J.* **2009**, *45*, 3269.
6. Schrenk, W. J. U.S. Pat. 3,773,882 (**1973**).
7. Schell, T. A.; Pockat, G. R.; Lischefski, A. J. E.P. Pat. 1,396,337 (**2013**).
8. Gámez-Pérez, J.; Santana, O. O.; Gordillo, A.; Maspoch, M. L. *Polym. Eng. Sci.* **2007**, *47*, 1365.
9. Affdl, J.; Kardos, J. *Polym. Eng. Sci.* **1976**, *16*, 344.
10. Kolarik, J. *Polym. Eng. Sci.* **1996**, *36*, 2518.
11. Kolarik, J. *Eur. Polym. J.* **1998**, *34*, 585.
12. Shin, E.; Hiltner, A.; Baer, E. *J. Appl. Polym. Sci.* **1993**, *47*, 269.
13. Kerns, J.; Hsieh, A.; Hiltner, A.; Baer, E. *J. Appl. Polym. Sci.* **2000**, *77*, 1545.
14. Haderski, D.; Sung, K.; Im, J.; Hiltner, A.; Baer, E. *J. Appl. Polym. Sci.* **1994**, *52*, 121.
15. Ching, E. C. Y.; Li, R. K. Y.; Tjong, S. C.; Mai, Y. W. *Polym. Eng. Sci.* **2003**, *43*, 558.
16. Broberg, K. *Int. J. Fract.* **1968**, *4*, 11.
17. Mai, Y. W.; Cotterell, B.; Horlyck, R.; Vigna, G. *Polym. Eng. Sci.* **1987**, *27*, 804.
18. Mai, Y. W.; Cotterell, B. *Int. J. Fract.* **1986**, *32*, 105.
19. Karger-Kocsis, J.; Moskala, E. *Polymer* **2000**, *41*, 6301.
20. Karger-Kocsis, J.; Barany, T.; Moskala, E. *Polymer* **2003**, *44*, 5691.
21. Karger-Kocsis, J.; Barany, T. *Polym. Eng. Sci.* **2002**, *42*, 1410.
22. Kim, H. S.; Karger-Kocsis, J. *Acta Mater.* **2004**, *52*, 3123.
23. Ching, E. C. Y.; Li, R. K. Y.; Mai, Y. W. *Polym. Eng. Sci.* **2000**, *40*, 310.
24. Ferrer-Balas, D.; Maspoch, M. L.; Mai, Y. W. *Polymer* **2002**, *43*, 3083.
25. Wong, J. S. S.; Ferrer-Balas, D.; Li, R. K. Y.; Mai, Y. W.; Maspoch, M. L.; Sue, H. *J. Acta Mater.* **2003**, *51*, 4929.
26. Sun, X.; Shen, H.; Xie, B.; Yang, W.; Yang, M. *Polymer* **2011**, *52*, 564.
27. Gong, G.; Xie, B.; Yang, W.; Li, Z.; Zhang, W.; Yang, M. *Polym. Test.* **2005**, *24*, 410.
28. Arkhireyeva, A.; Hashemi, S. *Polymer* **2002**, *43*, 289.
29. Wong, J. *Acta Mater.* **2003**, *51*, 4929.
30. Ganß, M.; Satapathy, B. K.; Thunga, M.; Weidisch, R.; Pötschke, P.; Jehnichen, D. *Acta Mater.* **2008**, *56*, 2247.
31. Bárány, T.; Czigány, T.; Karger-Kocsis, J. *Prog. Polym. Sci.* **2010**, *35*, 1257.
32. Sadeghi, F.; Ajji, A.; Carreau, P. *J. Polym. Eng. Sci.* **2007**, *47*, 1170.
33. Tabatabaei, S. H.; Carreau, P. J.; Ajji, A. *Polymer* **2009**, *50*, 3981.
34. Tabatabaei, S. H.; Carreau, P. J.; Ajji, A. *J. Membr. Sci.* **2009**, *345*, 148.
35. Maspoch, M. L.; Gámez-Pérez, J.; Gordillo, A.; Sánchez-Soto, M.; Velasco, J. I. *Polymer* **2002**, *43*, 4177.
36. Li, Z.; Yang, W.; Huang, R.; Fang, X.; Yang, M. *Macromol. Mater. Eng.* **2004**, *289*, 426.
37. van Veen, B.; van der Voort Maarschalk, K.; Bolhuis, G. K.; Frijlink, H. W. *Powder Technol.* **2004**, *139*, 156.
38. He, G.; Li, J.; Zhang, F.; Lei, F.; Guo, S. *Polymer* **2014**, http://dx.doi.org/10.1016/j.polymer.2014.01.039.
39. Hashemi, S. *Polym. Eng. Sci.* **2000**, *40*, 132.